

1 Article

2 An Improved Synthesis of Key Intermediate to the 3 Formation of selected Indolin-2-ones Derivatives 4 Incorporating Ultrasound and Deep Eutectic Solvent 5 (DES) Blend of Techniques, for some Biological 6 Activities and Molecular Docking Studies

7 MohdImran¹, Md. AfrozBakht^{2*}, Abida, Md. T. Alam¹, ElHassaneAnouar², Mohammed B.
8 Alshammari², NoushinAjmal³, ArchanaVimal⁴, Awanish Kumar⁴ and YassineRiadi⁵

9 ¹ Department of Pharmaceutical Chemistry, Faculty of Pharmacy, Northern Border University, Rafha 91911,
10 P.O. Box 840 Kingdom of Saudi Arabia; M. I (imran_inderlok@yahoo.co.in); A(aqua_abkhan@yahoo.com)
11 M. T. A. (tauquirpharm@gmail.com)

12 ² Department of Chemistry, College of Science and Humanities in Al-Kharj, Prince Sattam Bin Abdulaziz
13 University, Al-Kharj 11942, Saudi Arabia; M. A. B. (m_afroz007@yahoo.com); E. A
14 (anouarelhassane@yahoo.fr); M. B. A. (m.alshammari@psau.edu.sa)

15 ³ Department of Basic Sciences and Humanities, Pratap University, Jaipur, 303104, Rajasthan, India; N. A
16 (noush.biochem04@gmail.com)

17 ⁴ Department of Biotechnology, National Institute of Technology Raipur C. G., India; A. V
18 (avimal.phd2013.bt@nitrr.ac.in); A. K (awanik.bt@nitrr.ac.in)

19 ⁵ Department of Pharmaceutical Chemistry, College of Pharmacy, Prince Sattam Bin Abdulaziz University,
20 Al-Kharj 11942, Saudi Arabia; Y. R (yassinriadi@yahoo.fr)

21

22

23 * Correspondence: m_afroz007@yahoo.com;

24 Received: date; Accepted: date; Published: date

25 **Abstract:** We have developed a new idea to synthesize key intermediate molecule by utilizing deep
26 eutectic solvent (DES) and ultrasound in a multistep reaction to ensure process cost-effective. Key
27 intermediate (3) and final compounds (4a-n) were synthesized in a higher yield of 95% and
28 80-88% respectively. Further, final compounds (4a-n) were assessed for their anti-inflammatory,
29 analgesic, ulcerogenic and lipid peroxidation. The compounds 4f, 4g, 4j, 4l, and 4m showed good
30 anti-inflammatory activity, while 4f, 4i, and 4n exhibited very good analgesic activity as compared
31 to the standard drug. The ulcerogenicity of selected compounds was far less than the
32 indomethacin. The ligands had also shown a good docking score (4f = -6.859 and 4n = -7.077) as
33 compared to control indomethacin (-6.109). State-of-art DFT theory was used to validate the lipid
34 peroxidation mechanism of the active compounds which was in good agreement with the
35 variations of BDEs and IP of the tested compounds.

36 **Keywords:** Thiazole-indole; DES; Ultrasound; anti-inflammatory; analgesic; ulcerogenic; lipid
37 peroxidation; molecular docking; DFT.

38

39 1. Introduction

40 Non-steroidal anti-inflammatory drugs (NSAIDs) are a profound application for the treatment
41 of inflammatory diseases and pain. The NSAIDs are the choice of treatment in various inflammation
42 and pain related problems such as osteoarthritis, rheumatoid arthritis, spondylitis and gout [1-3]. A
43 mechanism based action of these drugs are exerted through the inhibition of cyclooxygenase type of

44 enzymes, a principal enzyme which is used in the conversion of arachidonic acid to
45 prostaglandin[4-6]. It has been reported that two forms of cyclooxygenase are involved in the
46 pathogenesis of pain and inflammation, COX-1 and COX-2[7,8]. However, their regulation and
47 expression in the body are different[8,9] COX-1 is known constitutive enzyme which helps in
48 cytoprotection in the gastrointestinal tract (GI). The inhibition COX-1 produces the undesired side
49 effects of NSAIDs, for example, gastrointestinal toxicity because of their ulcerogenic effects. The
50 COX-2 is an inducible enzyme that works through the mediation of the selective inflammatory
51 signal and the therapeutic anti-inflammatory action of NSAIDs is produced by the inhibition of
52 COX-2[10-14]. Based on this observation, many selective COX-2 inhibitors like celecoxib, rofecoxib,
53 and valdecoxib emerged as relatively safe NSAID'S together with improved gastric problems.
54 However, the reporting of the cardiovascular side effects, for example, increased risk of myocardial
55 infarction, stroke, heart failure and hypertension caused the withdrawal of many COX-2 inhibitors
56 from the market[15]. This encouraged researchprofessional to develop newer chemical entities as
57 anti-inflammatory agents with minimal side effects.

58 Indole ring and its derivatives have emerged as privileged pharmacophore representing more
59 than thousands natural isolates with known biological and pharmaceutical activities such as
60 anti-inflammatory and analgesic activity [16-19], antimicrobial activity [20], antitumor activity [21]
61 and anticonvulsant activity [22]. This ring is also a vital part of indomethacin, which is currently
62 marketed as NSAIDs. However, the gastric safety profile of indomethacin is not promising and it
63 produces gastrointestinal toxicity because of its ulcerogenic effects. In recent times, research reports
64 highlighting the usefulness of the development of new coumarinylthiazoles as an anti-inflammatory
65 agent and analgesic agents have also been published [23-25]. Thiazole and indole type of moieties
66 were reported to synthesize by utilizing harsh chemicals/solvents which causes environmental
67 pollution as well as raise the risk of health issues[26,27]. An alternative to such solvents such as deep
68 eutectic solvent (DES) is the most valuable choice for varieties of organic transformations [28, 29].
69 DES is usually a mixture of compounds having melting points less than their mixing components.
70 The most versatile DES was prepared from choline chloride and some hydrogen bond donor (urea,
71 glycerol) [29]. Depression in the melting point of DES is associated with molecular interaction of
72 choline chloride and hydrogen bond donor part [29].

73 Immense application of ultrasound has been highlighted recently in organic and material
74 science [30-31]. Ultrasound increased the rate of reaction by acoustic cavitation phenomena
75 generated as a result of initiation, growth and collapse of bubbles during the course of reactions.

76 Keeping these things and with extended work [32-35] of our group to the development of new
77 chemical templates in order to discover novel NSAIDs, authors planned to synthesize some
78 molecules with a low budget and utilizing deep eutectic solvent and ultrasound technique to fulfill
79 green chemistry approach.

80 **2. Results and discussion**

81 This section may be divided by subheadings. It should provide a concise and precise
82 description of the experimental results, their interpretation as well as the experimental conclusions
83 that can bedrawn.
84

85 2.1. Chemistry

86 1-(Substitutedphenylaminomethyl)-3-(2-(4-(2-oxochroman-3-yl)thiazol-2-yl)hydrazono)indolin
87 -2-ones were synthesized by treating 3-(2-(4-(2-oxochroman-3-yl) thiazol-2-yl) hydrazono)
88 indolin-2-one (**3**) with substituted aromatic amines and formaldehyde in ethylene glycol as depicted
89 in Figure 1. Prepared compounds were elucidated by FT-IR, ¹H-NMR, ¹³C-NMR, mass and elemental
90 analysis. In general, absorption bands due to two –NH group appeared in the IR spectra at around
91 3200 cm⁻¹. Other bands due to –C=N and two –C=O functional groups were found at around 1600
92 cm⁻¹ and 1700cm⁻¹, respectively. In the ¹H-NMR spectra, two –NH peak appeared at around 9 and 10
93 ppm. The lower value provides information as a singlet due to –NH attached as –CH₂NH with
94 indolinone nitrogen as a characteristic peak. Value at δ 5 ppm confirms the presence of –CH₂ which
95 is another important peak for identification. Further, characteristics peak of –CH₂ of –CH₂NH was
96 confirmed by ¹³C-NMR around δ 69 ppm.

97 The characterization data of all the synthesized compounds are provided below.

98
99 2-(2-Oxoindolin-3-ylidene)hydrazine carbothioamide (**2**): M.P.: 222-224 °C; %Yield: 72; IR (KBr)
100 cm⁻¹: 3413, 3352 and 3216 (N-H), 1693 (C=O).¹H-NMR (CDCl₃, DMSO-d₆) ppm: 6.72 (s, 1H, NH), 6.92
101 (d, J=12Hz, 1H, Ar-H), 7.03 (t, J=8Hz, 1H, Ar-H), 7.34 (t, J=8Hz, 1H, Ar-H), 8.04 (d, J=12Hz 1H, Ar-H),
102 9.99 (s, 1H, NH), 10.55 (s, 2H, NH); Elemental Analysis: Calcd. For (C₉H₈N₄O₅S), Found % (Calculated
103 %): C, 49.07 (49.08); H, 3.65 (3.66); N, 25.43 (25.44).

104 3-(2-(4-(2-Oxo-2H-chromen-3-yl)-4,5-dihydrothiazol-2-yl)hydrazono)indolin-2-one(**3**): M.P.:
105 240-242 °C; % Yield: 95; IR (KBr) cm⁻¹: 1692 and 1703 (C=O), 3315 and 3253 (N-H), 1612 (C=N), 1543
106 (C=C).¹H-NMR (CDCl₃, DMSO-d₆) ppm: 7.03 (t, J=8Hz, 1H, Ar-H), 7.39 (m, 8H, Ar-H, NH), 8.28 (s,
107 2H, Ar-H), 10.25 (s, 1H, -NH=N-); Elemental Analysis: Calcd. For (C₂₀H₁₂N₄O₅S), Found %
108 (Calculated %): C, 61.84 (61.85); H, 3.10 (3.11); N, 14.42 (14.43).

109 3-[[4-(2-Oxo-2H-chromen-3-yl)-thiazol-2-yl]-hydrazono]-1-phenylaminomethyl-1,3-dihydro-in
110 dol-2-one (**4a**): M.P.: 245-247 °C; %Yield: 85; IR (KBr) cm⁻¹: 1683 and 1710 (C=O), 3309 and 3251 (N-H),
111 1613 (C=N), 1546 (C=C); ¹H-NMR (CDCl₃, DMSO-d₆) ppm: 5.13 (s, 2H, CH₂), 7.44-8.10 (m, 13H,
112 Ar-H), 9.35 (s, 1H, NH), 10.53 (s, 1H, NH); ¹³C-NMR (125 MHz, DMSO-d₆): 171.0 (C=N,
113 thiazolidine), 159 and 162 (2CO), 156 (1C, C=N), 143.4, 140.9, 139.07, 139.0, 138.6, 131.0, 129.8, 129.5,
114 127.8, 126.8, 125.5, 124.3, 123.4, 121.2, 117.1, 112.4, (Ar-C), 69.3 (1C, CH₂); Elemental Analysis: Calcd.
115 For (C₂₇H₁₉N₅O₅S), Found % (Calculated %): C, 65.70 (65.71); H, 3.87 (3.88); N, 14.18 (14.19). Mass
116 (m/z): 493 (M⁺, C₂₇H₁₉N₅O₅S), 200 (C₁₁H₆NOS), 175 (C₁₀H₇OS), 168 (C₁₂H₁₀N), 159 (C₈H₇N₄), 132
117 (100%, C₇H₆N₃), 106 (C₇H₈N).

118 1-[[4-(4-Fluoro-phenylamino)-methyl]-3-[[4-(2-oxo-2H-chromen-3-yl)-thiazol-2-yl]-hydrazono]-1,3
119 -dihydro-indol-2-one (**4b**): M.P.: 242-244 °C; %Yield: 82; IR (KBr) cm⁻¹: 1683 and 1704 (C=O), 3312 and
120 3264 (N-H), 1613 (C=N), 1543 (C=C); ¹H-NMR (CDCl₃, DMSO-d₆) ppm: 5.10 (s, 2H, CH₂), 7.42 (m,
121 14H, Ar-H), 9.15 (s, 1H, NH), 10.55 (s, 1H, NH); ¹³C-NMR (125 MHz, DMSO-d₆): 172.0 (C=N,
122 thiazolidine), 160 and 161 (2CO), 155 (1C, C=N), 145.2, 143.1, 140.2, 139.0, 138.4, 132.5, 130.7, 129.3,
123 128.9, 127.6, 125.3, 124.4, 122.2, 118.3, 114.3, (Ar-C), 68.9 (1C, CH₂); MS (m/z): 511 (M⁺), 513 (M⁺+2);
124 Elemental Analysis: Calcd. For (C₂₇H₁₈N₅O₅SF), Found % (Calculated %): C, 63.38 (63.40); H, 3.55
125 (3.55); N, 13.68 (13.69).

126 1-[[4-(4-Chloro-phenylamino)-methyl]-3-[[4-(2-oxo-2H-chromen-3-yl)-thiazol-2-yl]-hydrazono]-1,
127 3-dihydro-indol-2-one (**4c**): M.P.: 233-235 °C; %Yield: 85; IR (KBr) cm⁻¹: 1689 and 1705 (C=O), 3309
128 and 3251 (N-H), 1613 (C=N), 1544 (C=C); ¹H-NMR (CDCl₃, DMSO-d₆) ppm: 5.14 (s, 2H, CH₂), 7.39
129 (m, 14H, Ar-H), 9.25 (s, 1H, NH), 10.50 (s, 1H, NH); ¹³C-NMR (125 MHz, DMSO-d₆): 170.0 (C=N,
130 thiazolidine), 161 and 162 (2C, C=O), 157 (1C, C=N), 146.1, 143.1, 140.3, 139.1, 138.6, 133.5, 131.7,
131 129.2, 128.4, 127.7, 126.3, 125.2, 123.1, 117.9, 112.8, (Ar-C), 68.6 (1C, CH₂); MS(m/z): 528 (M⁺), 530
132 (M⁺+2); Elemental Analysis: Calcd. For (C₂₇H₁₈N₅O₅SCl), Found % (Calculated %): C, 61.41 (61.42); H,
133 3.44 (3.44); N, 13.25 (13.26).

134 1-[[4-(4-Bromo-phenylamino)-methyl]-3-[[4-(2-oxo-2H-chromen-3-yl)-thiazol-2-yl]-hydrazono]-1,
135 3-dihydro-indol-2-one (**4d**): M.P.: 241-243 °C; %Yield: 80; IR (KBr) cm⁻¹: 1685 and 1704 (C=O), 3313
136 and 3251 (N-H), 1611 (C=N), 1547 (C=C); ¹H-NMR (CDCl₃, DMSO-d₆) ppm: 5.14 (s, 2H, CH₂), 7.40 (m,

137 14H, Ar-H), 9.30 (s, 1H, NH), 10.51 (s, 1H, NH); ¹³C-NMR (125 MHz, DMSO-d₆); 171.0 (C=N,
138 thiazolidine), 162 and 163 (2C, C=O), 156 (1C, C=N), 145.5, 143.6, 140.3, 139.8, 138.3, 133.6, 131.4, 129.7,
139 128.1, 127.7, 126.9, 123.6, 118.9, 112.9, (Ar-C), 69.3 (1C, CH₂); MS(m/z): 572 (M⁺), 574 (M⁺⁺²);
140 Elemental Analysis: Calcd. For (C₂₇H₁₈N₅O₃SBr), Found % (Calculated %): C, 56.64 (56.65); H, 3.16
141 (3.17); N, 12.22 (12.23).

142
143 1-[(2-Nitro-phenylamino)-methyl]-3-[[4-(2-oxo-2H-chromen-3-yl)-thiazol-2-yl]-hydrazono]-1,3-dihy
144 dro-indol-2-one (**4e**): M.P.: 244-246 °C; %Yield: 85; IR (KBr) cm⁻¹: 1684 and 1705 (C=O), 3310 and
145 3255 (N-H), 1613 (C=N), 1543 (C=C); ¹H-NMR (CDCl₃, DMSO-d₆) ppm: 5.07 (s, 2H, CH₂), 7.42 (m,
146 14H, Ar-H), 9.15 (s, 1H, NH), 10.48 (s, 1H, NH); ¹³C-NMR (125 MHz, DMSO-d₆); 170.0 (C=N,
147 thiazolidine), 163 and 164 (2CO), 157 (1C, C=N), 146.4, 143.8, 141.6, 140.4, 139.7, 135.6, 133.4, 130.7,
148 128.5, 127.5, 126.4, 124.6, 118.6, 112.3, (Ar-C), 70.1 (1C, CH₂); MS (m/z): 538 (M⁺), 540 (M⁺⁺²);
149 Elemental Analysis: Calcd. For (C₂₇H₁₈N₆O₅S), Found % (Calculated %): C, 60.21 (60.22); H, 3.36
150 (3.37); N, 15.60 (15.61).

151 1-[(2-chloro-phenylamino)-methyl]-3-[[4-(2-oxo-2H-chromen-3-yl)-thiazol-2-yl]-hydrazono]-1,3
152 -dihydro-indol-2-one (**4f**): M.P.: 239-241 °C; %Yield: 83; IR (KBr) cm⁻¹: 1689 and 1707 (C=O), 3311 and
153 3252 (N-H), 1613 (C=N), 1545 (C=C); ¹H-NMR (CDCl₃, DMSO-d₆) ppm: 5.10 (s, 2H, CH₂), 7.36 (m,
154 14H, Ar-H), 9.36 (s, 1H, NH), 10.55 (s, 1H, NH); ¹³C-NMR (125 MHz, DMSO-d₆); 172.0 (C=N,
155 thiazolidine), 161 and 162 (2CO), 157 (1C, C=N), 146.5, 143.9, 140.8, 140.1, 138.7, 135.4, 133.7, 129.7,
156 128.8, 127.6, 126.3, 124.7, 119.3, 114.1, (Ar-C), 68.3 (1C, CH₂); Elemental Analysis: Calcd. For
157 (C₂₇H₁₈N₅O₃SCl), Found % (Calculated %): C, 61.41 (61.42); H, 3.43 (3.44); N, 13.25 (13.26). Mass
158 (m/z): 527 (M⁺, C₂₇H₁₈N₅O₃SCl), 528 (M⁺¹), 202 (C₁₂H₉NCl), 175 (C₁₀H₇OS), 132 (100%, C₇H₆N₃), 111
159 (C₆H₄Cl), 59 (C₂H₃S).

160 1-[(2,4-Dinitro-phenylamino)-methyl]-3-[[4-(2-oxo-2H-chromen-3-yl)-thiazol-2-yl]-hydrazono]-
161 1,3-dihydro-indol-2-one (**4g**): M.P.: 247-249 °C; %Yield: 80; IR (KBr) cm⁻¹: 1686 and 1704 (C=O), 3292
162 and 3252 (N-H), 1612 (C=N), 1544 (C=C); ¹H-NMR (CDCl₃, DMSO-d₆) ppm: 5.15 (s, 2H, CH₂), 7.45 (m,
163 13H, Ar-H), 9.33 (s, 1H, NH), 10.51 (s, 1H, NH); ¹³C-NMR (125 MHz, DMSO-d₆); 169.0 (C=N,
164 thiazolidine), 159 and 161 (2CO), 155 (1C, C=N), 145.7, 142.5, 140.2, 139.1, 137.4, 135.7, 133.5, 129.6,
165 128.6, 127.3, 124.7, 118.9, 112.3, (Ar-C), 69.7 (1C, CH₂); MS(m/z): 583 (M⁺), 585 (M⁺⁺²); Elemental
166 Analysis: Calcd. For (C₂₇H₁₇N₇O₇S), Found % (Calculated %): C, 55.56 (55.57); H, 2.94 (2.94); N, 16.79
167 (16.80).

168 3-[[4-(2-Oxo-2H-chromen-3-yl)-thiazol-2-yl]-hydrazono]-1-([1,2,4]triazol-4-ylaminomethyl)-1,3-
169 dihydro-indol-2-one (**4h**): M.P.: 236-238 °C; %Yield: 80; IR (KBr) cm⁻¹: 1685 and 1706 (C=O), 3253 and
170 3279 (N-H), 1613 (C=N), 1543 (C=C); ¹H-NMR (CDCl₃, DMSO-d₆) ppm: 5.17 (s, 2H, CH₂), 7.48 (m,
171 12H, Ar-H), 9.42 (s, 1H, NH), 10.47 (s, 1H, NH); ¹³C-NMR (125 MHz, DMSO-d₆); 170.0 (C=N,
172 thiazolidine), 161 and 161 (2CO), 157 (1C, C=N), 144.8, 140.2, 137.4, 135.9, 132.4, 129.4, 128.7, 127.5,
173 124.3, 116.9, 112.3, (Ar-C), 70.2 (1C, CH₂); MS(m/z): 484 (M⁺), 486 (M⁺⁺²); Elemental Analysis: Calcd.
174 For (C₂₃H₁₆N₈O₃S), Found % (Calculated %): C, 57.01 (57.02); H, 3.32 (3.33); N, 23.12 (23.13).

175
176 1-[(3-Chloro-4-fluoro-phenylamino)-methyl]-3-[[4-(2-oxo-2H-chromen-3-yl)-thiazol-2-yl]-hydrazono
177]-1,3-dihydro-indol-2-one (**4i**): M.P.: 246-248 °C; %Yield: 85; IR (KBr) cm⁻¹: 1684 and 1703 (C=O), 3240
178 and 3273 (N-H), 1612 (C=N), 1544 (C=C); ¹H-NMR (CDCl₃, DMSO-d₆) ppm: 5.05 (s, 2H, CH₂), 7.41 (m,
179 13H, Ar-H), 9.31 (s, 1H, NH), 10.55 (s, 1H, NH); ¹³C-NMR (125 MHz, DMSO-d₆); 171.0 (C=N,
180 thiazolidine), 161 and 163 (2CO), 156 (1C, C=N), 146.9, 143.4, 140.6, 139.2, 137.6, 135.7, 133.8, 129.3,
181 128.3, 127.6, 124.2, 117.4, 112.3, (Ar-C), 68.6 (1C, CH₂); MS(m/z): 546 (M⁺), 548 (M⁺⁺²); Elemental
182 Analysis: Calcd. For (C₂₇H₁₇N₅O₃SClF), Found % (Calculated %): C, 59.38 (59.40); H, 3.14 (3.14); N,
183 12.82 (12.83).

184 3-[[4-(2-Oxo-2H-chromen-3-yl)-thiazol-2-yl]-hydrazono]-1-(pyridine-4-ylaminomethyl)-1,3-dih
185 ydro-indol-2-one (**4j**): M.P.: 237-239 °C; %Yield: 88; IR (KBr) cm⁻¹: 1687 and 1705 (C=O), 3244 and 3268
186 (N-H), 1613 (C=N), 1545 (C=C); ¹H-NMR (CDCl₃, DMSO-d₆) ppm: 5.17 (s, 2H, CH₂), 7.45 (m, 14H,
187 Ar-H), 9.38 (s, 1H, NH), 10.57 (s, 1H, NH); ¹³C-NMR (125 MHz, DMSO-d₆); 172.0 (C=N, thiazolidine),
188 161 and 163 (2CO), 156 (1C, C=N), 144.8, 143.5, 140.4, 139.0, 138.3, 132.5, 130.9, 129.3, 128.8, 127.6,

189 125.1,124.7, 122.9, 116.9, 112.6, (Ar-C), 68.3(1C, CH₂); MS (m/z): 594 (M⁺), 596 (M⁺+2); Elemental
190 Analysis: Calcd. For (C₂₆H₁₈N₆O₃S), Found % (Calculated %): C, 63.14 (63.15); H, 3.66 (3.67); N, 16.98
191 (16.99).

192 3-[[4-(2-Oxo-2H-chromen-3-yl)-thiazol-2-yl]-hydrazono]-1-(pyridine-3-ylaminomethyl)-1,3-dih
193 ydro-indol-2-one (**4k**):M.P.: 231-233 °C; %Yield: 85; IR (KBr) cm⁻¹: 1686 and 1706 (C=O), 3251 and
194 3277 (N-H), 1612 (C=N), 1543 (C=C); ¹H-NMR (CDCl₃, DMSO-d₆) ppm: 5.15 (s, 2H, CH₂), 7.47 (m,
195 14H, Ar-H), 9.35 (s, 1H, NH), 10.55 (s, 1H, NH); ¹³C-NMR (125 MHz, DMSO-d₆); 172.0 (C=N,
196 thiazolidine),161 and 162 (2CO), 156 (1C, C=N),144.9, 143.6, 140.2, 139.0, 138.5, 132.3,130.7, 129.5,
197 128.7, 127.3, 125.5,124.9, 122.8, 116.6, 112.4, (Ar-C), 68.3(1C, CH₂); MS (m/z): 594 (M⁺), 596 (M⁺+2);
198 Elemental Analysis: Calcd.For(C₂₆H₁₈N₆O₃S), Found % (Calculated %): C, 63.14 (63.15); H, 3.66 (3.67);
199 N, 16.98 (16.99).

200 1-[(4-Nitro-phenylamino)-methyl]-3-[[4-(2-oxo-2H-chromen-3-yl)-thiazol-2-yl]-hydrazono]-1,3-
201 dihydro-indol-2-one (**4l**):M.P.: 241-243 °C; %Yield: 90; IR (KBr) cm⁻¹: 1684 and 1702 (C=O), 3255 and
202 3278 (N-H), 1612 (C=N), 1544 (C=C); ¹H-NMR (CDCl₃, DMSO-d₆) ppm: 5.18 (s, 2H, CH₂), 7.46 (m,
203 14H, Ar-H), 9.32 (s, 1H, NH), 10.54 (s, 1H, NH); ¹³C-NMR (125 MHz, DMSO-d₆); 170.0 (C=N,
204 thiazolidine), 163 and 164 (2CO), 158 (1C, C=N), 146.6, 143.7, 141.9, 140.5, 139.7, 135.2, 133.5, 130.1,
205 128.2, 127.7, 126.1, 124.3, 116.9, 112.3, (Ar-C), 70.2(1C, CH₂); MS (m/z): 538 (M⁺), 540 (M⁺+2);
206 Elemental Analysis: Calcd. For (C₂₇H₁₈N₆O₅S), Found % (Calculated %): C, 60.21 (60.22); H, 3.36
207 (3.37); N, 15.60 (15.61).

208 3-[[4-(2-Oxo-2H-chromen-3-yl)-thiazol-2-yl]-hydrazono]-1-(p-tolylamino-methyl)-1,3-dihydro-i
209 ndol-2-one (**4m**): M.P.: 244-246 °C; %Yield: 84; IR (KBr) cm⁻¹: 1685 and 1706 (C=O), 3252 and 3273
210 (N-H), 1608 (C=N), 1544 (C=C); ¹H-NMR (CDCl₃, DMSO-d₆) ppm: 2.23 (s, 3H, CH₃), 5.11 (s, 2H, CH₂),
211 7.41 (m, 14H, Ar-H), 9.31 (s, 1H, NH), 10.48 (s, 1H, NH); ¹³C-NMR (125 MHz, DMSO-d₆); 172.0 (C=N,
212 thiazolidine), 160 and 163 (2CO), 156 (1C, C=N), 146.8, 144.2, 142.4, 140.6, 139.9, 135.3, 133.8, 130.5,
213 128.8, 127.1, 126.3, 124.8, 117.4, 114.1, (Ar-C), 70.3(1C, CH₂); MS (m/z): 507 (M⁺), 509 (M⁺+2);
214 Elemental Analysis: Calcd. For (C₂₈H₂₁N₅O₃S), Found % (Calculated %): C, 66.25 (66.26); H, 4.16
215 (4.17); N, 13.79 (13.80).

216 3-[[4-(2-Oxo-2H-chromen-3-yl)-thiazol-2-yl]-hydrazono]-1-(o-tolylamino-methyl)-1,3-dihydro-i
217 ndol-2-one (**4n**):M.P.: 237-239 °C; %Yield: 86; IR (KBr) cm⁻¹: 1686 and 1703 (C=O), 3251 and 3282
218 (N-H), 1612 (C=N), 1543 (C=C); ¹H-NMR (CDCl₃, DMSO-d₆) ppm: 2.21 (s, 3H, CH₃), 5.13 (s, 2H,
219 CH₂), 7.43 (m, 14H, Ar-H), 9.34 (s, 1H, NH), 10.53 (s, 1H, NH); ¹³C-NMR (125 MHz, DMSO-d₆); 171.0
220 (C=N, thiazolidine), 161 and 162 (2CO), 157 (1C, C=N), 145.9, 144.2, 142.6, 140.3, 139.2, 135.6, 133.5,
221 130.2, 128.9, 127.6, 126.1, 124.9, 118.2, 112.3, (Ar-C), 68.3(1C, CH₂); Elemental Analysis: Calcd. For
222 (C₂₈H₂₁N₅O₃S), Found % (Calculated %): C, 66.25 (66.26); H, 4.16 (4.17); N, 13.80 (13.80); Mass (m/z):
223 507 (M⁺, C₂₈H₂₁N₅O₃S), 387 (C₂₀H₁₁N₄O₃S), 200 (C₁₁H₆NOS), 132 (100%, C₇H₆N₃), 120 (C₈H₁₀N), 90
224 (C₆H₄N), 59 (C₂H₃S).

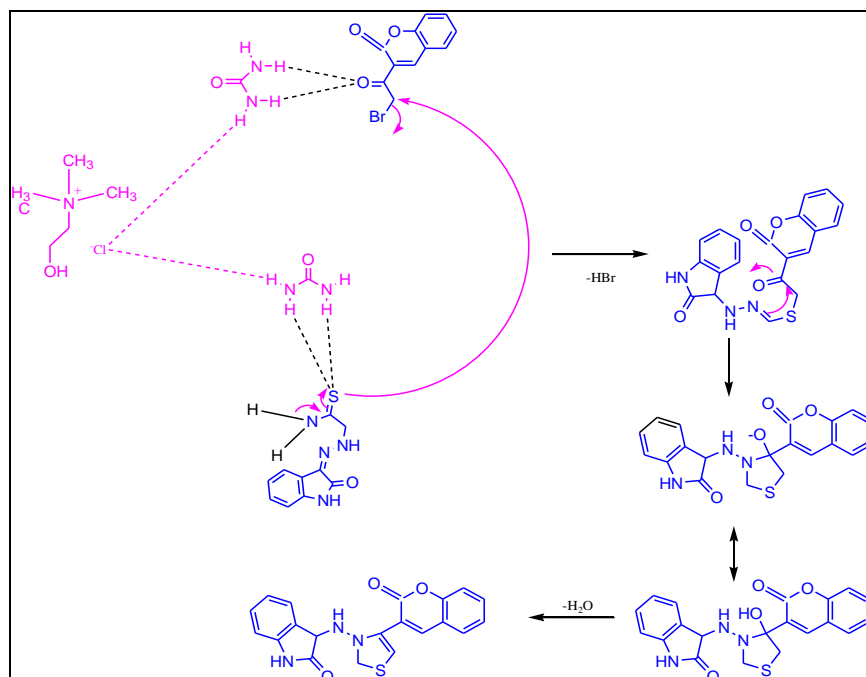
225 2.1.1. Significance of DES and ultrasound blend of techniques to the synthesis of key intermediate
226 3-(2-(4-(2-oxochroman-3-yl) thiazol-2-yl) hydrazono) indolin-2-one

227 To develop the efficient method as compared to conventional, we have conducted the synthesis
228 of key intermediate (3) utilizing biocompatible deep eutectic solvent (DES) and ultrasound blend of
229 technique. As a result of combined use of DES and ultrasound, there have been found an increase in
230 % yield of key intermediate as high as 95% with the expense of 1hr only. Whereas, a similar type of
231 organic transformations using dioxane and another organic solvent together with conventional
232 heating were reported to have % yield around 44-68% in 3-4 hr [36-38]. Further, we have also found
233 80-88% of all final compounds (4a-n) utilizing ultrasound as a source of heating. Some of our earlier
234 work and other related literature also mentioned the significance DES and ultrasound technology as
235 an energy saving process [29, 39, 40] which is certainly a good favor of our present work.

236 2.1.2. Plausible mechanism involved to the formation of key intermediate,3-(2-(4-(2
237 -oxochroman-3-yl)thiazol-2-yl) hydrazono) indolin-2-one

238 The exact mechanism of formation of the desired intermediate compound is not yet clear. But it
 239 was suggested by some researchers that urea part of DES (Choline chloride: urea, 1:2) catalyze the
 240 reaction by making hydrogen bond. Thus, urea in deep eutectic solvent involved to stabilize the
 241 acetyl moiety of 3-bromoacetyl coumarin via hydrogen bonding, which was further attacked by
 242 amide functional group of hydrazine thioamide to form key intermediate, 3-(2-(4-
 243 (2-oxochroman-3-yl) thiazol-2-yl) hydrazono) indolin-2-one through cyclization and dehydration
 244 process (Scheme 1).

245



246 **Scheme 1.** Proposed mechanism involved to the formation of key intermediate,
 247 3-(2-(4-(2-oxochroman-3-yl) thiazol-2-yl) hydrazono) indolin-2-one using DES.

248 Moreover, ultrasound also played a significant role in the formation of the desired compound.
 249 Under the influence of sonic waves inside the reaction vessel, there was the formation of microscopic
 250 bubbles, as a result of high temperature and pressure [28-31]. These tiny microscopic bubbles also
 251 help in the cyclization process.

252 2.2. Biology

253 2.2.1. Anti-inflammatory activity

254 Anti-inflammatory activity of the synthesized compounds (4a-n) was evaluated by
 255 carrageenan-induced paw edema method. An oral dose of 10mg/kg was used for compounds and
 256 compared with the standard. Anti-inflammatory activity was accessed through percentage
 257 inhibition after 2h and 4h (Table 1).

258

259

260

261

262

263

264

265

266

Table 1. Antiinflammatory activity of 1-(Substituted phenyl amino methyl)-3-(2-(4-(2-oxochroman-3-yl) thiazol-2-yl) hydrazono) indolin-2-one (4a-n).

Compound	% age inhibition of rat paw edema(Dose = 10 mgkg-1)		Potency
	2 Hour	4 Hour	
Indomethacin	66.34 ± 0.051	82.05 ± 0.08	1.00
4a	38.29 ± 0.016	5.57 ± 0.041	0.06
4b	59.29 ± 0.73*	45.81 ± 0.069	0.55
4c	59.29 ± 0.143*	30.17 ± 0.294	0.36
4d	51.92 ± 0.337	6.98 ± 0.315	0.08
4e	62.24 ± 0.080**	48.60 ± 0.090**	0.59
4f	48.377 ± 0.219*	72.42 ± 0.183*	0.88
4g	53.57 ± 0.160*	77.94 ± 0.184***	0.94
4h	35.39 ± 0.273	64.69 ± 0.245	0.78
4i	31.268 ± 0.188	63.95 ± 0.218	0.77
4j	53.81 ± 0.120**	77.906 ± 0.171**	0.94
4k	38.095 ± 0.214	70.75 ± 0.165	0.86
4l	54.76 ± 0.228**	80.94 ± 0.149***	0.98
4m	53.27 ± 0.183*	78.42 ± 0.183**	0.95
4n	42.57 ± 0.213	69.58 ± 0.133	0.84

267

*p < 0.05, **p < 0.01, ***p < 0.001.

268

269

270

271

Anti-inflammatory activity in terms of percentage inhibition for the test compounds are ranging from 5.57% to 80.94 % (Table1), whereas standard drug showed 82.05% after 4 hours. Compounds 4f (72.42%), 4g (77.94%), 4j (77.90%), 4k (70.75%), 4l (80.94%) and 4m (78.42%) showed comparable results against the standard drug.

272

273

274

275

276

277

278

279

280

281

282

283

284

The structure of 1-(Substituted phenyl amino methyl)-3-(2-(4-(2-oxochroman-3-yl) thiazol-2-yl) hydrazono) indolin-2-one derivatives revealed that the compound 4l (Ar = 4-nitrophenyl) exhibited highest anti-inflammatory activity. Other compounds of the series, namely, 4f (Ar = 2-chlorophenyl), 4g (Ar = 2,4-dinitrophenyl), 4j (Ar = 4-pyridyl), 4k (Ar = 2-pyridyl) and 4m (Ar = 4-methyl phenyl) also displayed significant anti-inflammatory activity. Two compounds, 4a (Ar = phenyl) and 4d (Ar = 4-bromophenyl) displayed negligible anti-inflammatory activity. All other compounds displayed moderate anti-inflammatory activity. Further, the number and position of substituents also count the variation in anti-inflammatory activity. Nitrogen bearing compounds 4g (Ar = 2,4-dinitrophenyl) and 4l (Ar = 4-nitrophenyl) showed highest anti-inflammatory activity. When chloro substituent present on ortho-position(4f) of phenyl ring displayed almost double activity as compared to a compound bearing parachloro compound (4c). Similarly, the difference in anti-inflammatory activity was found in compounds 4j & 4k and 4m & 4n due to different arrangements of substituents on the phenyl ring.

285

2.2.2. Analgesic activity

286

287

Compounds under investigation showed analgesic activity ranging from 7.96% to 69.36% with reference drug of 73.61% (Table 2).

288

289

290

291

292

293

294

Table 2. Analgesic activity of 1-(Substituted phenyl amino methyl)-3-(2-(4-(2-oxochroman-3-yl)thiazol-2-yl) hydrazono)indolin-2-one (4a-n).

Compound	Mean writhe \pm SEM	% Analgesic Activity (Dose = 10 mg/kg-1)	Potency
Indomethacin	8.55 \pm 0.394	73.61 \pm 0.315*	1.00
4a	17.00 \pm 0.2582	47.54 \pm 0.7071*	0.64
4b	24.00 \pm 0.3651	25.94 \pm 0.5802**	0.35
4c	13.00 \pm 0.2582	59.88 \pm 0.8458*	0.81
4d	18.50 \pm 0.4282	42.91 \pm 0.710***	0.58
4e	16.88 \pm 0.222	47.91 \pm 1.0049*	0.65
4f	9.93 \pm 0.386	69.36 \pm 0.5845*	0.94
4g	20.09 \pm 0.3561	38.01 \pm 1.0035**	0.51
4h	23.83 \pm 0.3073	26.47 \pm 0.3165*	0.35
4i	10.93 \pm 0.3128	66.27 \pm 1.0072*	0.90
4j	17.13 \pm 0.539	47.14 \pm 0.4018***	0.64
4k	29.83 \pm 0.3073	7.96 \pm 0.4318*	0.10
4l	17.83 \pm 0.3079	44.98 \pm 0.3361*	0.61
4m	21.83 \pm 0.2051	32.64 \pm 0.8454**	0.44
4n	10.00 \pm 0.3651	69.14 \pm 0.6892*	0.93

295

* $p < 0.05$, ** $p < 0.01$, *** $p < 0.001$.

296

297

298

299

300

301

302

All the tested compounds and standard drug are evaluated at 10mg/kg oral dose. It was identified that compound (4l) showed maximum anti-inflammatory activity produces least analgesic activity, but some selected compounds like- 4f, 4i and 4n displayed analgesic activity in a similar fashion as anti-inflammatory activity (Table1, Table 2). Compound (4k) exhibited the least analgesic activity was among the top-ranked anti-inflammatory activity. On the contrary, many of compounds exhibited good analgesic properties were not displayed good anti-inflammatory activity and vice-versa (Table 1, Table 2).

303

304

305

306

307

308

309

310

311

312

313

After a close understanding of anti-inflammatory and analgesic potentials of compounds under present series, we have made a structure-activity relationship. Compounds possessing a substituted phenyl ring showed better anti-inflammatory and analgesic activity than a compound having an unsubstituted phenyl ring. In most of the cases, the substitution of electron withdrawing groups at C-2 and C-4 positions of phenyl ring resulted in potent compounds except compound 4d (Ar = 4-bromophenyl) that showed negligible anti-inflammatory activity. Compound 4i possessing two electron withdrawing groups exhibited moderate anti-inflammatory activity but good analgesic activity. Compound (4m) having an electron releasing group (-CH₃) at C-4 position exhibited better anti-inflammatory activity but less analgesic activity. On the other hand, a methyl group at C-2 showed better anti-inflammatory and analgesic agent (4n). A steep decrease in analgesic activity was observed when the phenyl ring was replaced by a triazole ring (4h).

314

2.2.3. Acute ulcerogenicity

315

316

317

318

319

Four compounds, namely, 4c (Ar = 4-chlorophenyl), 4f (Ar = 2-chlorophenyl), 4i (Ar = 4-fluoro-3-chlorophenyl) and 4n (Ar = 2-methylphenyl) were selected for their ulcerogenic activity. This selection was based on their anti-inflammatory and analgesic activity. Compounds were evaluated at oral dose of 30mg/kg relative to 10mg/kg indomethacin.

320
321**Table 3.**Ulcerogenic activity and lipid peroxidation of 1-(Substituted phenyl amino methyl)-3-(2-(4-(2-oxochroman-3-yl) thiazol-2-yl) hydrazono)indolin-2-one.

Compound	Severity Index	Nanomoles of MDA
		content \pm SEM/ 100 mg tissue
Control	0.0	3.16 \pm 0.12*
Indomethacin	4.500 \pm 0.316	6.71 \pm 0.18*
4c	0.666 \pm 0.105*	4.26 \pm 0.12*
4f	0.666 \pm 0.105*	4.08 \pm 0.22*
4i	0.500 \pm 0.129	3.89 \pm 0.17*
4n	0.833 \pm 0.210*	4.81 \pm 0.13*

322

* $p < 0.05$

323 The ulcerogenic activity of these compounds revealed that all the compounds showed a lesser
324 severity index for ulcerogenicity than indomethacin (Table 3). Compound 4n exhibited the highest
325 severity index of 0.833 but it was only 20% of the severity shown by the standard. Mainly
326 compounds, 4f, 4i and 4n displayed excellent anti-inflammatory, an analgesic with reduced
327 ulcerogenic potential. Significant reduction in ulcerogenicity is ranging from 0.500 \pm 0.129 to
328 0.833 \pm 0.210, whereas standard drug indomethacin showed a high severity index of 4.500 \pm 0.316.

329 2.2.4. Lipid peroxidation

330 Gastrointestinal (GI) ulceration, bleeding and renal problems are common complications of
331 NSAID'S consumption, which is directly related to lipid peroxidation. It has been evidenced that
332 drug having less ulcerogenicity showed reduced malondialdehyde (a byproduct of lipid
333 peroxidation) content[4, 41]. We have examined the lipid peroxidation (LP) of compounds which
334 exhibited maximum anti-inflammatory and analgesic activities (4c, 4f, 4i, 4n). It was measured as
335 nmol of MDA/100mg of gastric tissue. We have found lipid peroxidation value maximum 6.71 \pm 0.18
336 for indomethacin, whereas 3.89 \pm 0.17, 4.08 \pm 0.22, 4.26 \pm 0.12 and 4.81 \pm 0.13 for compounds 4i, 4c, 4f and
337 4n respectively. It was interesting to mention that all these compounds having electron withdrawing
338 functionality on the phenyl ring (except 4n) exhibited less ulcerogenicity with reduced lipid
339 peroxidation (Table 3).

340 2.2.5. DFT results

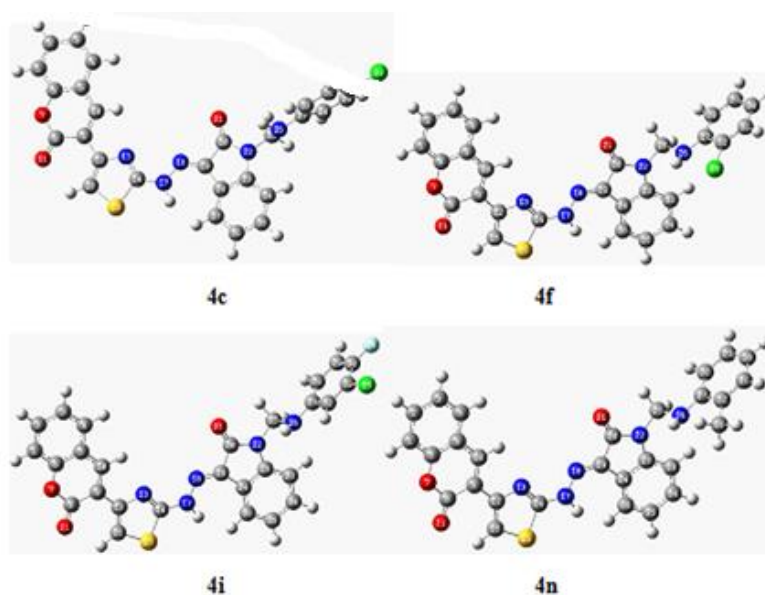
341 As mentioned above, only the synthesized derivatives (In-H) that exhibited maximum
342 anti-inflammatory and analgesic activities derivatives are subjected to lipid peroxidation (LP) test
343 (Table 4, Figure 1). The tested In-H derivatives show the ability to scavenge LOO• free radical. To
344 shed light on the small observed lipid peroxidation inhibition of In-H derivatives, bond dissociation
345 enthalpies of the of i-NH function groups and ionization potential energies of the tested compounds
346 and were calculated at the B3P86/6-311+G (d,p) level of theory (Table 4 and Figure 3).

347 **Table 4.**BDEs (kcal/mol) of i-NH groups of the In-H synthesized derivatives and its corresponding
348 ionization potential energies calculated at the B3P86/6-31+G(d,p) level of theory.

Compound	IP (eV)	17-NH	26-NH	Lipid peroxidation
				Inhibition
4c	-5.96	62.03	72.58	4.08 \pm 0.22
4f	-5.97	62.08	75.60	4.26 \pm 0.12
4i	-6.04	62.05	72.84	3.89 \pm 0.17
4n	-5.80	62.05	72.02	4.81 \pm 0.13

349

350 The tested compounds showed similar lipid peroxidation with a small variation between their
351 values. This result is confirmed by the small differences of BDEs of the active 17-NH group and IP
352 energies, where the maximum variations of BDEs and IPs are of 0.03 kcal/mol and 0.08 eV,
353 respectively.



354 **Figure 1.** The optimized structure with numbering of In-H synthesized derivatives.

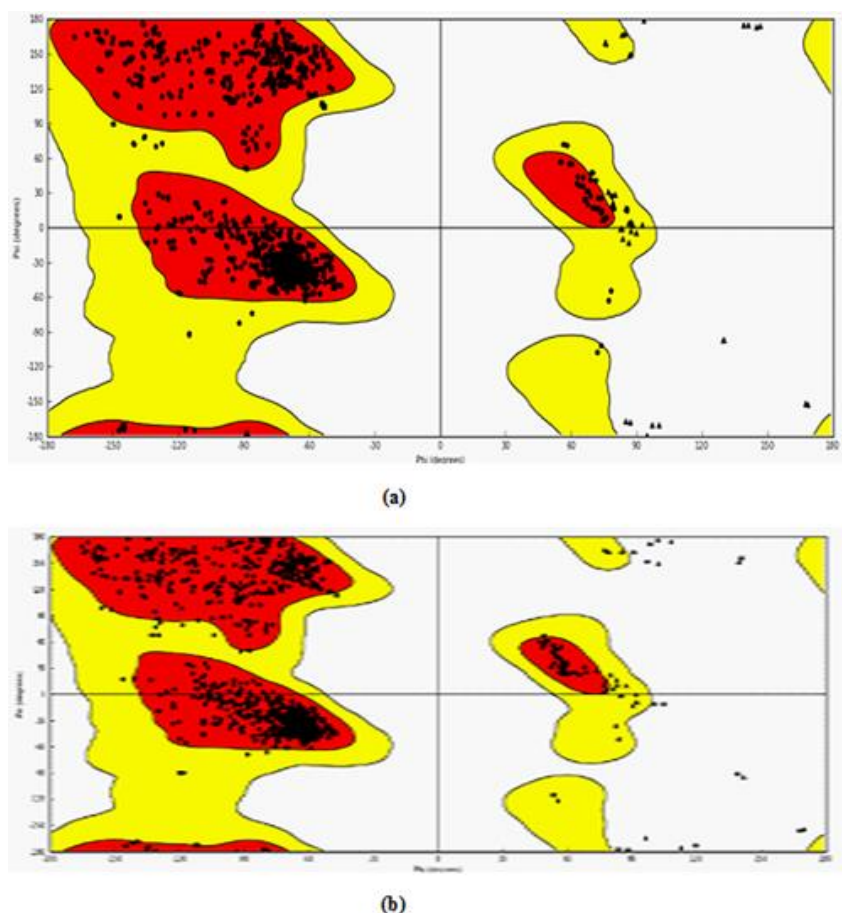
355 2.2.6. *In-Silico* study

356 2.2.6.1. Target protein selection and retrieval

357 The target protein COX-2 from two different organisms i.e. mouse and human are retrieved
358 from protein data bank having PDB id 3NT1 and 5F91 respectively [42-43].

359 2.2.6.2. Protein (COX-2) preparation and validation

360 The protein structures obtained from PDB were modified suitably for the docking studies. The
361 modified protein structures were validated through the Ramachandran plot. The Ramachandran
362 plot of these two target protein is shown in Figure 2 (a) and (b).

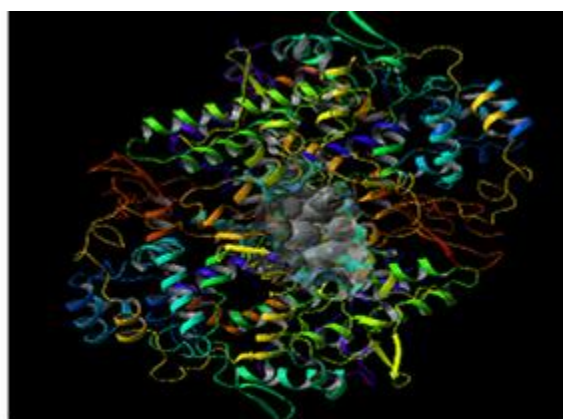


363 **Figure 2.** The binding site predicted where ligand is docked in COX-2 from (a) mouse (PDB ID 3NT1)
 364 (b) human (PDB ID : 5F19).

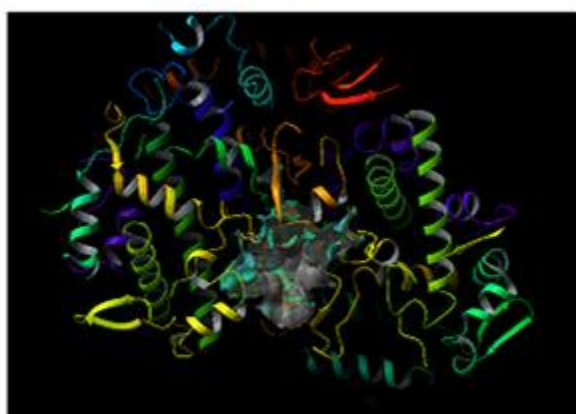
365 The evaluation of phi/psi angles validates the protein structure as most of the residues are in the
 366 most favored region. In case of 3NT1, 90.8% amino acid residues are in the most favored regions
 367 whereas 8.8%, 0.1%, and 0.3% are in additional allowed regions, generously allowed regions and
 368 disallowed regions respectively. Similarly, in 5F91 90.7%, 9.1%, 0.1%, and 0.1% amino acid residues
 369 are in the most favored regions, additionally allowed regions, generously allowed regions and
 370 disallowed regions respectively. The result obtained allows the use of these structures for further
 371 docking studies.

372 2.2.6.3. Prediction and evaluation of the binding site in COX-2

373 The Site map application predicts five different drug binding sites in both the target proteins.
 374 The site score for the protein 3NT1 were 1.078, 1.053, 1.048, 1.034 and 0.991. Similarly, the site score
 375 obtained for the protein 5F19 was 1.082, 1.051, 1.046, 1.034 and 0.990. As a rule of thumb binding site
 376 having a score above are considered as druggable pockets. In the present *in-silico* study site with the
 377 highest score were selected for the docking studies. The druggable pocket inside the respective
 378 target proteins is shown in Figure 3 (a) 3NT1 and (b) 5F19.



(a)



(b)

379 **Figure3.**The binding site predicted where ligand is docked in COX-2 from (a) mouse (PDB ID 3NT1)
380 (b) human (PDB ID : 5F19)

381 2.2.6.4. Ligand Preparation

382 The lowest energy conformation of each test ligands (4a-4n) was prepared for the docking
383 studies as per the standard guidelines and used in the molecular docking studies.

384 2.2.6.5. Grid Generation in the target protein COX-2

385 After the determination of the exact location of the drug binding site in each target, protein grid
386 was generated around the binding sites to specify the volume and location of the druggable pocket.

387 2.2.6.6. Molecular docking studies

388 Table 5. Summary of molecular docking score of different ligands against Cox-2 (target protein)
389 from mouse (3NT1) and human (5F19).

390

391

392

393

394

395

396

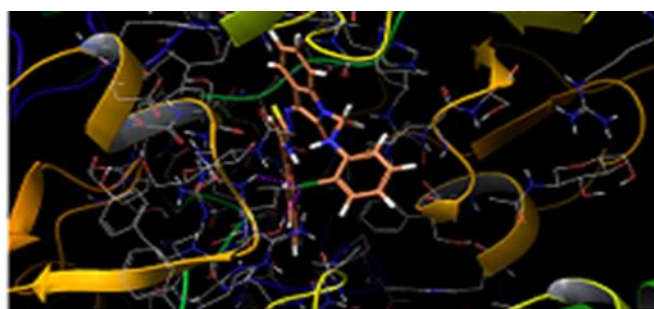
397
398**Table 5.** Summary of molecular docking score of different ligands against Cox-2 (target protein) from mouse (3NT1) and human (5F19).

S. No	Ligand	Docking Score		Emodel Score		Energy	
		Mouse	Human	Mouse	Human	Mouse	Human
1	4a	-7.050	-6.834	-84.018	-85.694	-59.395	-60.236
2	4b	-8.552	-7.398	-93.570	-91.718	-61.736	-63.562
3	4c	-6.847	-7.368	-89.139	-90.888	-65.402	-63.532
4	4d	-6.271	-7.419	-86.746	-90.209	-64.531	-63.856
5	4e	-6.995	-7.200	-88.939	-90.453	-63.810	-64.065
6	4f	-6.071	-6.859	-78.327	-79.342	-58.256	-59.290
7	4g	-7.247	-7.426	-92.213	-92.642	-65.665	-64.682
8	4h	-8.422	-7.760	-99.511	-97.487	-65.199	-66.691
9	4i	-7.242	-7.446	-92.293	-93.023	-64.084	-64.835
10	4j	-8.120	-7.250	-97.069	-89.953	-64.452	-62.022
11	4k	-7.887	-7.261	-94.176	-90.861	-63.958	-63.245
12	4l	-8.447	-7.544	-95.832	-81.672	-65.289	-56.454
13	4m	-7.898	-6.803	-85.845	-84.328	-59.419	-60.257
14	4n	-6.693	-7.077	-85.842	-87.991	-62.568	-61.802
15	Indomethacin	-6.324	-6.109	-57.309	-58.132	-39.727	-40.695

399

400 Present series (4a-n) undergo docking studies using Glide (version 7.0) application of the
 401 Schrodinger Maestro interface. All the derivatives of 1-(substituted phenyl amino
 402 methyl)-3-(2-(4-(2-oxochroman-3-yl) thiazol-2-yl) hydrazono) indolin-2-ones were docked to the
 403 active site of the target enzyme COX-2 (PDB ID: 3NT1 and 5F19). These compounds were
 404 compared with the reference drug (Indomethacin), considering docking score, E-model score and
 405 binding energy against mouse (3NT1) and human (5F19) model (Table 5).

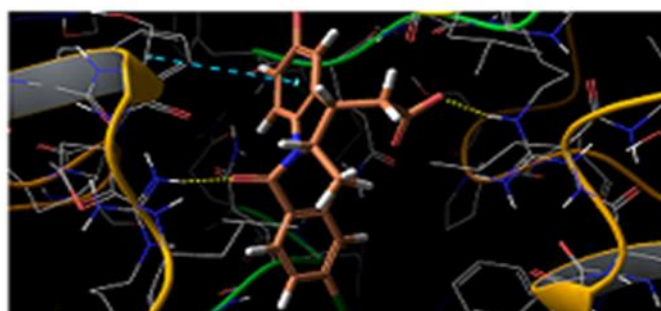
406 The maximum test ligands that are 4 a, b, c, e, g, h, i, j, k, l, m, n showed docking score lower
 407 than the control/reference drug (-6.324) against the mouse target protein. A similar pattern of
 408 docking score is observed against human target protein where all test ligands 4 a-n have lower
 409 docking score as compared to control having a score -6.109. It was believed that low binding energy
 410 dock conformer exhibited maximum stability. The two best compound on the basis of experimental
 411 results that are 4n and 4f have docking score -7.077 and -6.859 against human target protein
 412 respectively. The same two ligand 4n and 4f have a score -6.693 and -6.071 against mouse target
 413 protein respectively. The docked ligands (4n and 4f) inside the binding pocket of the respective
 414 target proteins (3NT1 and 5F19) is shown in figure 4 and figure 5.



(a) 4f



(b) 4n



(c) Indomethacin

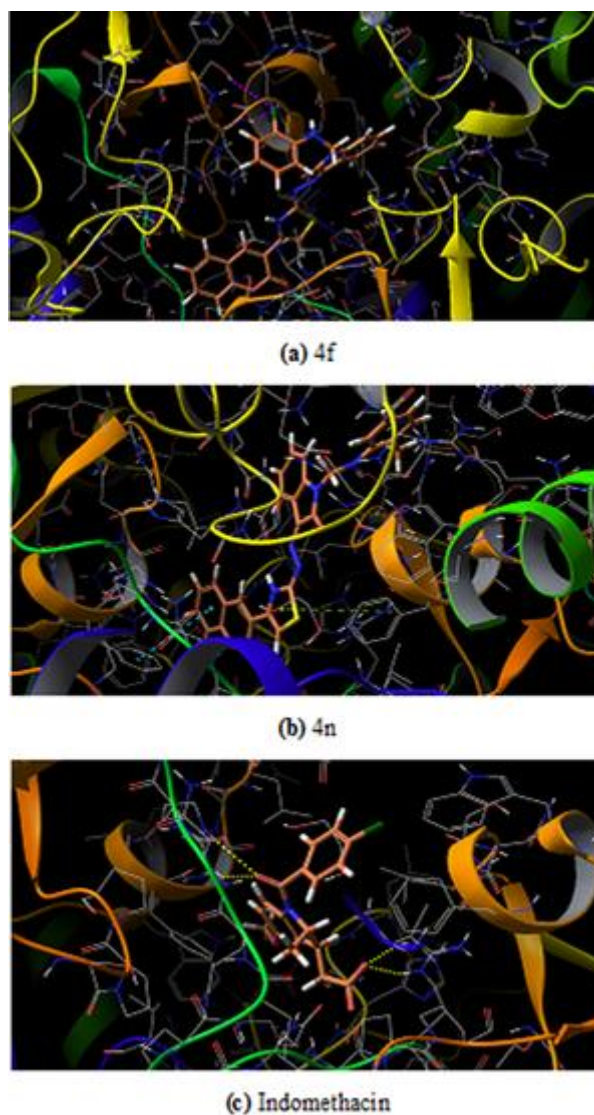
415

416

417

418

Figure 4. Docked ligand inside the binding pocket of COX-2 from mouse (a) 4f (b) 4n (c) Indomethacin.



419

420

421

Figure 5. Docked ligand inside from the binding pocket of COX-2 from human (a) 4f (b) 4n (c) Indomethacin.

422

423

424

425

The further efficacy of the docking is interpreted in the terms interaction that exists between the ligand and the surrounding amino acid residues inside the druggable pocket. The overall binding interaction (in terms of bonding) for each ligand is summarized in Table 6 and Table 7 for the proteins 3NT1 and 5F19 respectively.

426

427

428

429

430

431

432

433

434 **Table 6.**Types of interaction and amino acid residues involve in that interaction inside the
 435 binding pocket of Cox- 2 from mouse (4NT1).

S. No	Ligand	Types of Interaction	Interacting Residues
1	4a	Solvation effect	-
2	4b	1 H-bond, 1 pi-pi stacking	Phe 142, Asn 37
3	4c	1 pi-pi stacking	Phe 142
4	4d	1 H-bond, 1 pi-pi stacking	Trp, 139, Phe, 142
5	4e	2 H-bond	Leu 145, Ser 146
6	4f	Solvation effect	-
7	4g	2 H-bond	Leu 145, Ser 146
8	4h	1 H-bond, 1 pi-pi stacking	Phe 142, Gly 225
9	4i	2 pi-pi stacking	Phe 142, Arg 133
10	4j	3 H-bond	Glu 142, Arg 376
11	4k	1 pi-pi stacking	Phe 142
12	4l	3 H-bond, 1 pi-pi stacking	Phe 142, Val 228, Asn 375, Asn 537
13	4m	1 H-bond, 1 pi-pi stacking	Phe 142, Asn 375
14	4n	2 H-bond	Arg 376
15	Indomethacin	2 H-bond, 1 pi-pi stacking	Phe 142, Arg 376

436

437 **Table 7.**Types of interaction and amino acid residues involve in that interaction inside the binding
 438 pocket of Cox- 2 from mouse (5F19).

S. No	Ligand	Types of Interaction	Interacting Residues
1	4a	1 pi-pi stacking	Phe 142
2	4b	2 pi-pi stacking	Phe 142, Arg 333
3	4c	2 pi-pi stacking	Phe 142, Arg 333
4	4d	2 pi-pi stacking	Phe 142, Arg 333
5	4e	2 H-bond	Leu 145, Ser 146
6	4f	Solvation effect	-
7	4g	3 H-bonds	Leu 145, Ser 146, Nag 605
8	4h	2 H-bond, 1 pi-pi stacking	Arg 333, Arg 376
9	4i	2 pi-pi stacking	Phe 142, Arg 333
10	4j	2 H-bond	Glu140, Arg 376
11	4k	1 H-bond, pi-pi stacking	Trp 139, Phe 142, Arg 333
12	4l	2 H-bond, 2 pi-pi stacking	Phe 142, Gln 241, Arg 333
13	4m	2 pi-pi stacking	Phe 142, Arg 333
14	4n	2 pi-pi stacking	Phe 142, Arg 333
15	Indomethacin	2 H-bonds	Arg 376

439 Among the two potent ligands, 4n is more suitable for drug candidate as it possesses a strong affinity
 440 towards the target proteins. In 3NT1 it forms two hydrogen bonds with Arg 376, whereas in 5F19
 441 two pi-pi stacking exists with the involvement of Phe 142 and Arg 333. In the case of 4f, there is no
 442 hydrogen bonding or pi-pi interaction is observed whether it is 3NT1 or 5F19. All these interactions
 443 are shown in figure 7 and figure 8 as ligand interaction diagram.

451 2.2.6.7. ADME profiling

452 The suitability of test ligands as drug candidate according to their pharmacokinetic behavior
453 was also assessed using *in silico* approach. Many drug candidates fail at a later stage due to their
454 poor pharmacokinetic performance. In order to avoid such failure and save time, energy and money
455 *in silico* ADME profiling is a good choice [44]. The result of *in silico* ADME profiling is presented in
456 Table 8 that suggests that values of test parameters are within the recommended range
457 (http://glab.cchem.berkeley.edu/glab/schrodinger_old/qikprop/qikprop_user_manual.pdf).

458 The oral drug absorption is predicted in terms of apparent Caco-2 permeability (QPplogCaco)
459 that represents the gut-blood barrier. The value above 500 indicates a great absorption while below
460 25 is considered a poor score [44]. The ligand 4n and 4f have QPplogCaco value 619.284 and 479.473
461 that is very good as compared to indomethacin that has the score of 185.783 only. The Madin-Darby
462 canine kidney (MDCK) cell model is used to investigate the apparent MDCK cell permeability[45].
463 The score above 500 is considerably good that is obtained in both the test ligand cases. The score for
464 4n and 4f are 586.303 and 809.359 whereas the standard drug has a value of 251.855. The percent
465 human abortion of both the potential ligand is also comparable to the standard and above 80%. The
466 test ligands are also found to be following Lipinski rule of 5.

467 5.1.1.4. Statistical analysis

468 Data used in the experimental pharmacological section was used as the mean \pm standard error of
469 the mean (SEM). One way analysis of variance (ANOVA) and Dennett's multiple comparison test
470 techniques was employed to compare between test, control and standard group, utilizing statistical
471 software Graph pad prism version 5.00. Such results showed significantly different at $p < 0.05$

472

Table 8. ADMET profiling of different ligands synthesized to be used as drug candidate.

S. No	Ligand	Mol. Wt.	QPlogPo/w (Octanol/Water)	apparent Caco-2 permeability (QPP Caco)	brain/blood partition coefficient (QPlogBB)	apparent MDCK permeability (QppMDCK)	Human oral absorption % (QP%)	Lipinski rule of 5 violations (Rule of 5)
1	4a	493.539	5.757	574.519	-1.128	540.552	100	1
2	4b	511.529	5.966	521.054	-1.100	880.621	84.589	2
3	4c	527.984	6.226	521.126	-1.051	1201.640	86.113	2
4	4d	572.435	6.306	521.273	-1.043	1292.410	86.581	2
5	4e	538.536	4.878	85.123	-2.223	59.380	64.132	2
6	4f	527.984	6.047	479.473	-1.121	809.359	84.417	2
7	4g	583.534	4.121	10.166	-3.511	5.971	43.182	2
8	4h	484.491	2.102	23.583	-1.616	18.982	50.863	1
9	4i	545.974	6.468	578.335	-0.889	2174.980	88.336	2
10	4j	494.927	4.735	329.574	-1.421	3.000	100	0
11	4k	494.927	4.703	313.043	-1.444	296.440	100	0
12	4l	538.536	5.003	68.904	-2.393	54.611	50.266	3
13	4m	507.566	6.083	574.067	-1.164	540.037	86.024	2
14	4n	507.566	6.027	619.284	-1.085	586.303	86.288	2
15	Indomethacin	373.835	3.679	185.783	-0.614	251.855	89.095	0

474 **3. Materials and Methods**

475 Melting points were evaluated in open capillary tubes and are uncorrected. 5PC FT-IR
476 spectrometer (Brower Morner, USA), Bruker DRX-300 FT NMR (Bruker, Germany)
477 spectrophotometer and Jeol-JMS-D-300 mass spectrometer (70 eV) (Jeol, Japan) for IR, NMR and
478 mass respectively were used to characterize the compounds.

479 *3.1. Chemistry*480 *3.1.1. Preparation of 2-(2-oxoindolin-3-ylidene)hydrazinecarbothioamide (2)*

481 A combination of isatin (0.01 mole) and thiosemicarbazide (0.01 mole) was placed in 100 mL
482 round bottom flask with 50 mL of methanol as solvent and refluxed for 2 hours and then put onto
483 the ice. The obtained was filtered, dried and recrystallized using methanol.

484 *3.1.2. Preparation of deep eutectic solvent (DES)*

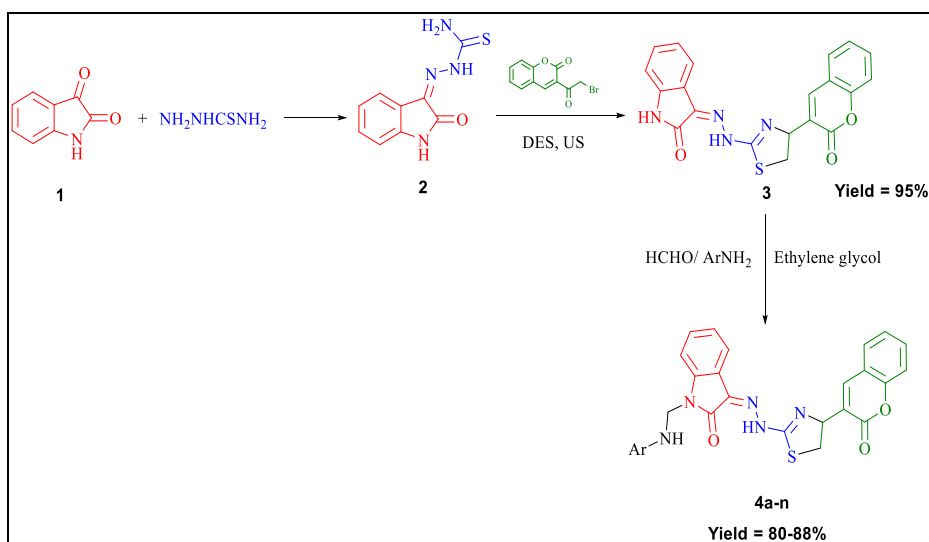
485 A mole ratio (1:2) of choline chloride and urea were chosen to prepare DES as per reported
486 method [28].

487 *3.1.3. Preparation of 3-(2-(4-(2-oxochroman-3-yl)thiazol-2-yl)hydrazono)indolin-2-one using deep*
488 *eutectic solvent and ultrasound (3)*

489 In a specially designed sonicating flask an equimolar(0.01mole) quantity of 3-bromoacetyl
490 coumarin and 2-(2-oxoindolin-3-ylidene) hydrazinecarbothioamide (2) with 8 g of prepared DES
491 was added. A sonicating probe of 26 kHz frequency at 40% amplitude was submerged into the
492 reaction vessel. Completion of the reaction was monitored by taking TLC in regular interval. Upon
493 completion, it was poured onto crushed ice. Upon completion of the reaction, it was extracted by
494 dichloromethane using separating funnel. Organic solvent layer was collected and evaporated to get
495 the desired product. DES was isolated and keeps for future use.

496 *3.1.4.*497 *Preparation of 1-(Substituted phenylaminomethyl)-3-(2-(4-(2-oxochroman-3-yl)thiazol-2-yl)hydrazono)*
498 *indolin-one (4a-n)*

499 A mixture of 3-(2-(4-(2-oxochroman-3-yl)thiazol-2-yl)hydrazono)indolin-2-one (3) (0.01 mole),
500 substituted aromatic amines (0.01 mole) and formaldehyde (0.02 moles) in 30 ml of ethylene glycol
501 was refluxed from 1 hour to 3 hours. The reaction mixture was transferred onto the crushed ice upon
502 completion, as confirmed by TLC. The solid decanted, filtered, washed with water, dried and
503 recrystallized from dioxane.
504



505

506

507

Scheme 2. Schematic representation of synthesis of compounds (4a-n) via key intermediate (3) isolated from deep eutectic solvent and ultrasound blend of technique.

508

3.2. Biology

509

3.2.1. Preparation of 2-(2-oxoindolin-3-ylidene)hydrazinecarbothioamide (2)

510

Compounds produced were assessed for their anti-inflammatory activity using the carrageenan-induced hind paw edema method [46]. The anti-inflammatory activity was carried out using Wistar albino rats of either sex (150-220 g) using Digital Plethysmometer (Model No. 7140, UGO BASILE). The edema was induced by using 1% carrageenan solution. Indomethacin was used as standard drug. The anti-inflammatory activity of the standard drug and tested compounds was determined at a dose of 10 mg/kg body weight. The animals were divided into groups containing 6 animals each and initial paw volume of each rat was noted by NaCl displacement method. One group was kept as control, one as standard and rest groups of the compounds to be tested. To the control group, 1% CMC solution was administered p.o. To the standard group, the standard drug was administered orally. To the test group, tested compounds were administered orally. After 60 minutes of the 1% CMC solution/standard drug/test compound administration, 0.1 ml of 1% (w/v) carrageenan was injected in the plantar region of the hind limb (right) of all the rats in each group including the control group. The paw volume was again measured after the time interval of 2 hours and 4 hours. Using the following formula, inflammation was calculated as percentage inhibition for the test and reference compounds

525

526

527

$$\left[\frac{\text{Final foot volume of control} - \text{Final foot volume of std. / test}}{\text{Final foot volume of control}} \right] \times 100$$

528

3.2.2. Analgesic activity

529

The analgesic activity of the tested compounds was carried out by acetic acid induced writhing method as given in the literature [9] using Swiss albino mice of either sex (25-35 g). The writhing were induced in the albino mice using an intraperitoneal injection of 1% acetic acid solution. The standard drug indomethacin and test compounds were evaluated at a concentration of 10 mg/kg of the body weight. The animals were divided into groups and each group consisted of 6 animals. One group was kept as control, one as standard and other as test groups. To the control group, 0.1% CMC solution was administered p.o.; to the standard group standard drug was administered orally, and to the test group test compounds were administered orally. After 60 minutes of the 0.1% CMC solution/standard drug / tested compound administration, 0.1 ml of 1% (v/v) acetic acid solution in distilled water was injected intraperitoneally of all the mice in each group including the control group. The writhing (contraction of the abdomen, turning of trunk and extension of hind limbs) was

539

540 counted after 5 minutes of acetic acid administration and were counted for a period of 15 minutes.
 541 The percentage of analgesic activity was calculated using the following formula.

$$542 \quad \quad \quad [(Mean\ wriths\ of\ control - Mean\ wriths\ of\ std./test) / Mean\ wriths\ of\ control] \times 100$$

544 3.2.3. Acute ulcerogenic activity

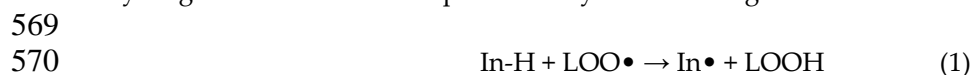
545 Acute ulcerogenic activity evaluation of the synthesized compounds was carried out according
 546 to the method described [47] using Wistar rats of either sex (180-220 g). The animals were distributed
 547 into control, group, and test group. Each group consisted of six rats. All the rats fasted for 24 hours
 548 with free access to water. To control group, 1% CMC solution was administered p.o; to the standard
 549 group indomethacin at a concentration of 20 mg/kg was administered orally; and to the test, groups
 550 tested compounds were administered orally at a concentration of 30 mg/kg. After the dose
 551 administration animals were kept for 17 hours. After this, the animals were sacrificed for the
 552 appraisal of ulcerogenic assessment. Stomach was taken out from the animal body and washed with
 553 flushing water, then with a cotton swab wetted with saline(0.9%) and pinned on wax coated try.
 554 Glandular portion of the stomach was cleaned again with saline to closely identify the presence of a
 555 type of ulcers or hemorrhage mark using a magnifying glass. The mucosal injury of the stomach was
 556 evaluated as per the following system: 0.5= redness.; 1=spot ulcer.; 1.5= hemorrhage streak.; 2=
 557 ulcers<3.; 3= ulcers>3<5. The value obtained as a result of the mean score of individual treated group
 558 - mean score of control is referred to as the severity index of the gastric mucosal damage.

559 3.2.4. Lipid peroxidation study

560 The method adopted for lipid peroxidation is same as of Ohkawa et al[48] and recent work of
 561 our researchers[9].

562 3.2.5. Theoretical details

563 It is well known that almost all phenolic compounds may inhibit lipid peroxidation process due
 564 to their ability to scavenge the chain-carrying lipid peroxy radicals, LOO•. The lipid, LH,
 565 peroxidation process is represented by three main steps initiation, propagation, and terminations.
 566 The scavenging of LOO• by the synthesized indolin-2-ones derivatives (In-H) may refer to
 567 hydrogen atoms transferred or an electron transfer from the former to the lipid peroxy radical. The
 568 hydrogen atom transfer is represented by the following reaction:



570
 571
 572 The above lipid peroxidation inhibition is governed by bond dissociation enthalpies (BDE) of
 573 i-NH groups of the synthesized indolin-2-ones derivatives (In-H). BDE is calculated using the
 574 following equation:

$$575 \quad \quad \quad BDE = [H(In\bullet, 298K) + H(H\bullet, 298K)] - H(In-H, 298K),$$

576
 577 where H is the enthalpy that considered as temperature-dependent corrections [zero point
 578 energy (ZPE), vibrational, rotational and translational energies at 298K; H(In•, 298K) and H(An-H,
 579 298K) are the enthalpies of In-H derivatives and its corresponding radical obtained after the
 580 homolytic bond dissociation of i-NH groups, respectively. H(H•, 298K) is the enthalpy of hydrogen
 581 radical. The minimum value of BDE indicates that hemolytic bond dissociation is much easier,
 582 which is helpful in lipid peroxidation process

583 Previously, we showed the success of the hybrid functional B3B86 in rationalizing the
 584 scavenging of free radical by synthesized and natural polyphenols [49-51]. Hence, we extended here
 585 the use of B3P86 to the In-H synthesized derivatives as lipid peroxy radical inhibitors. We have
 586 already tested, the basic set effect on BDEs of hispidin and isohispidin isomers by using varieties of
 587 basic sets. The obtained BDEs showed differences lower than 0.4 kcal/mol for active sites and a slight

588 influence on IP values [49]. Consequently, a double basis set, 6-31+G(d,p), was used in this study.
589 The 3D geometry optimization of In-H derivatives and their corresponding radicals In• were
590 performed at the B3P86/6-31+G(d,p) level of theory. The ground state minima were confirmed by
591 vibrational frequency calculations (i.e., the absence of imaginary frequencies). All DFT chemical
592 calculations have been performed using the mentioned methodology, as implemented in Gaussian
593 09 package [52].

594 3.2.6. *In-Silico* study

595 3.2.7. Software

596 The present *in silico* study that includes homology modeling of the target protein,
597 molecular docking, and ADME proofing was carried out using Schrodinger Maestro interface
598 (Maestro, version 10.5, Schrödinger, LLC, New York, NY, 2016)[53, 54].

599 3.2.8. Target protein selection and retrieval

600 In the present study, COX-2 is selected as the target protein since the therapeutic response of
601 NSAIDs is generated by blocking/inhibiting this enzyme. The 3-D structure of COX-2 was retrieved
602 from Protein Data Bank (PDB, <https://www.rcsb.org/>). There were two structures of this enzyme, one
603 from mouse and from human origin were obtained, having PDB ID 3NT1 and 5F91 respectively.

604 3.2.9. Protein (COX-2) preparation and validation

605 The 3-D structure of target proteins that are obtained from PDB was prepared (for further steps)
606 using the tool protein preparation sorcerer (version 4.3). The protein preparation is a multi-step
607 process that includes the addition of hydrogen atoms, optimization of hydrogen bonds, and
608 elimination of any atomic level clashes. The final step of protein preparation is energy minimization
609 that was performed at the condition 0.3 Å of RMSD and the OPLS_2005 force field[55].

610 The protein structures prepared in the above step were further validated through a
611 Ramachandran plot based on phi/psi angles evaluation.

612 3.2.10. Prediction and evaluation of the binding site in COX-2

613 To locate the position where ligands can bind to the target protein was predicted through Site
614 map application (version 3.8). The potency of the predicted site is decided on the basis of site score
615 generated by the tool.

616 The binding site effectiveness is determined by several physical parameters like size, the degree
617 of enclosure/exposure, hydrophobic/hydrophilic character, opportunities of hydrogen bonding, etc.

618 3.2.11. Ligand preparation

619 The derivatives of 1-(substituted phenyl amino methyl)-3-(2-(4-(2-oxochroman-3-yl) thiazol
620 -2-yl) hydrazono) indolin-2-ones (4a to 4n) that are synthesized chemically in the previous step are
621 used as ligands. The chemical structure of individual ligand was drawn and prepared using LigPrep
622 (version 3.7). The purpose of ligand preparation is to generate 3-D structure (of each ligand) with
623 minimum energy conformation.

624 3.2.12. Grid Generation in the target protein COX-2

625 The grid was created nearby the binding site in the respective target proteins that were
626 predicted in the previous step. It determines the exact position and size of the binding site in terms
627 of receptors grids that is required for the docking step. The box size taken is of 20×20×20 Å³ and
628 atoms were scaled by van der Waals radii of 1.0 Å having partial atomic charge less than 0.25.

629 3.2.13. Docking of ligands and COX-2

630 The prepared ligands were docked in the COX-2 (target protein) at the respective binding site
631 through Glide (version 7.0) application. The Extra precision (XP) algorithm was employed for the
632 docking operation and output is obtained in the form of docking score. It determines a possible
633 binding pose between the target and the ligand at the binding site along with the information about
634 the most favorable interactions among them[56-58].

635 3.2.14. ADME profiling

636 The test ligands i.e. the derivatives of 1-(substituted phenyl amino methyl)-3-(2-(4-
637 (2-oxochroman-3-yl)thiazol-2-yl)hydrazono)indolin-2-ones (4a to 4n) were assessed for their
638 pharmacokinetic efficacy through QikProp program (version 4.7). The tool predicts 51
639 pharmacokinetic properties but the present study includes a few important parameters that are logP
640 (Octanol/Water), apparent Caco-2 permeability (QPP Caco), brain/blood partition coefficient
641 (QPlogBB), apparent MDCK permeability (QppMDCK), (QP%) human oral absorption %, and
642 Lipinski rule of 5 violations (Rule of 5).

643 4. Conclusions

644 In conclusion, an improved synthesis of key intermediate through the combined use of deep
645 eutectic solvent and ultrasound is a rational approach to enhance the yield of desired compounds
646 via an economically viable and environmentally acceptable way. Further, all the final compounds
647 (4a-n) have been evaluated as anti-inflammatory and analgesic activities. Selected compounds were
648 further tested for ulcerogenic and lipid peroxidation potential. Only two compounds claimed to be
649 most potent as anti-inflammatory and analgesic molecule with the highest reduction in GI toxicity.
650 In silico study also supports the utility of these two potent ligands as drug candidate and paves the
651 path for future drug development studies. The active compounds showed similar lipid peroxidation
652 activities, and this mainly due to their closest BDEs and IP values, i.e., the active compounds have
653 the same potency to inhibit lipid radical by a hydrogen atom transfer from the active site of titled
654 compounds to a lipid radical.

655 **Author Contributions:** Conceptualization, Mohd Imran, Md. Afroz Bakht, Mohammed B.
656 Alshammari and Abida.; Synthesis of organic compounds, Mohd Imran, Md. Afroz Bakht and
657 Abida.; Preparation of DES, Yassine Riadi and Md. Afroz Bakht.; Biological activities, Mohd
658 Imran, Md. Afroz Bakht and Noushin Ajmal.; Characterization of organic compounds, Md. T. Alam,
659 Mohammed B. Alshammari, and Yassine Riadi.; Docking studies, Archana Vimal and Awanish.;
660 DFT studies, ElHassane Anouar.; Writing original draft and compilation of final draft, Mohd
661 Imran, Md. Afroz Bakht, Mohammed B. Alshammari and ElHassane Anouar.

662 **Funding:** "This research received no external funding"

663 **Acknowledgments:** One of the author (Mohd. Imran) is thankful to the Faculty of Pharmacy,
664 JamiaHamdard, New Delhi, India for providing research facility for synthesis and experimental
665 pharmacology. One of author thankful to Chemistry Department, College of science, Prince Sattam
666 Bin Abdulaziz University, Saudi Arabia for DFT results. We are also thankful to the Department of
667 Biotechnology, National Institute of Technology Raipur (CG), India for required docking studies.

668 **Conflicts of Interest:** The authors declare no conflict of interest.

669
670
671
672
673
674

675 **References**

- 676 1. Kumar, N.; Sharma, C.S.; Ranawat, M.S.; Singh, H.P.; Chauhan, L.S.; Dashora, N. Synthesis, analgesic
677 and anti-inflammatory activities of novel mannich bases of benzimidazoles. *J. Pharm. Invest.* **2015**, *45*,
678 65–71.
- 679 2. Almasirad, A.; Mousavi, Z.; Tajik, M.; Assarzadeh, M.J.; Shafiee, A. Synthesis, analgesic and
680 anti-inflammatory activities of new methyl-imidazolyl-1,3,4-oxadiazoles and 1,2,4-triazoles. *Daru J.*
681 *Pharm. Sci.* **2014**, *22*, 1–8.
- 682 3. Salgın-Gökşen, U.; Gökhan-Kelekçi, N.; Göktaş, Ö.; Köysal, Y.; Kılıç, E.; Işık, S.; Aktay, G.; Özalp,
683 M. 1-Acylthiosemicarbazides, 1,2,4-triazole-5(4H)-thiones, 1,3,4-thiadiazoles and hydrazones
684 containing 5-methyl-2-benzoxazolinones: synthesis, analgesic anti-inflammatory and antimicrobial
685 activities. *Bioorg. Med. Chem.* **2007**, *15*, 5738–5751.
- 686 4. Kumar, H.; Javed, S.A.; Khan, S.A.; Amir, M. 1,3,4-Oxadiazole/thiadiazole and 1,2,4-triazole
687 derivatives of biphenyl-4-yloxy acetic acid: Synthesis and preliminary evaluation of biological
688 properties. *Eur. J. Med. Chem.* **2008**, *43*, 2688–2698.
- 689 5. Marnett, L.J.; Kalgutkar, A.S. Cyclooxygenase 2 inhibitors: discovery, selectivity and the
690 future Trends. *Pharmacol. Sci.* **1999**, *20*, 465–469.
- 691 6. Marnett, L.J.; Kalgutkar, A.S. Design of selective inhibitors of cyclooxygenase-2 as non ulcerogenic
692 anti-inflammatory agents. *Curr. Opin. Chem. Biol.* **1998**, *2*, 482–90.
- 693 7. Parsit, P.; Reindeau, D. Selective Cyclooxygenase-2 Inhibitors. *Annu. Rep. Med. Chem.* **1997**, *32*, 211–20.
- 694 8. Almansa, C.; Alfon, J.; Cavalcanti, F.L.; Synthesis and Structure–Activity Relationship of a New Series
695 of COX-2 Selective Inhibitors: 1,5-Diarylimidazoles. *J. Med. Chem.* **2003**, *46*, 3463–3475.
- 696 9. Alafeefy, A.M.; Bakht, M.A.; Ganaie, M.A.; Ansarie, M.N.; NEL-Sayed, N.N.; Awaad, AS.; Synthesis,
697 analgesic, anti-inflammatory and anti-ulcerogenic activities of certain novel Schiff's bases as
698 fenamate isosteres. *Bioorg. Med. Chem. Lett.* **2015**, *25*, 179–183.
- 699 10. Kujubu, D.A.; Fletcher, B.S.; Varnuzu, B.; Lim, R.W.; Herschmann, H.R. TIS 10, a phorbol ester tumor
700 promotor-inducible mRNA from Swiss 3T3 cells encodes a novel prostaglandin
701 synthase/cyclooxygenase homologue. *J. Bio. Chem.* **1991**, *266*, 12866–12872.
- 702 11. Mitchell, J.A.; Akaraseenont, P.; Thiernemann, C.; Flower, R.J.; Vane, J.R.; Selectivity of
703 non-steroidal anti-inflammatory drugs as inhibitors of constitutive and inducible
704 cyclooxygenase. *Nat. Acad. Sci. USA.* **1993**, *90*, 11693–11697.
- 705 12. Laine, L. Nonsteroidal anti-inflammatory drug gastropathy. *Gastrointest. Endosc. Clin. N. Am.* **1996**,
706 *6*, 489–504.
- 707 13. Fries, J.F.; Williams, C.A.; Bloch, D.A.; The relative toxicity of nonsteroidal anti-inflammatory drugs.
708 *Arthr. Rheum.* **1991**, *34*, 1353–1360.
- 709 14. Gaba, M.; Singh, D.; Singh, S.; Sharma, V.; Gaba, P. Synthesis and pharmacological evaluation of
710 novel 5-substituted-1-(phenylsulfonyl)-2-methylbenzimidazole derivatives as anti-inflammatory and
711 analgesic agents. *Eur. J. Med. Chem.* **2010**, *45*, 2245–2249.
- 712 15. Zarghi, A.; Arfaei, S. Selective COX-2 inhibitors: A review of their structure-activity
713 relationships. *Iran. J. Pharm. Res.* **2011**, *10*, 655–683.
- 714 16. Sujatha, K.; Perumal, P.T.; Muralidharan, D.; Rajendran, M. Synthesis, analgesic and
715 anti-inflammatory activities of bi(indolyl) methanes. *Ind. J. Chem.* **2009**, *48B*, 267–272.
- 716 17. Nirmal, R.; Prakash, C.R.; Meenakshi, K.; Shanmugapandiyar, P. Synthesis and Pharmacological
717 Evaluation of Novel Schiff Base Analogues of 3-(4-amino) Phenylimino) 5-fluoroindolin-2-one. *J*
718 *.Young. Pharm.* **2010**, *2*, 162–168.
- 719 18. Chavan, R.S.; More, H.N.; Bhosale, A.V. Synthesis, Characterization and Evaluation of Analgesic and
720 Anti-inflammatory Activities of Some Novel Indoles. *Trop. J. Pharm. Res.* **2011**, *10*, 463–473.
- 721 19. Dubey, P.K.; Kumar, T.V.; Synthesis of [2-(3-oxo-3,4-dihydro-2H-benzo[1,4]
722 oxazin-6-carbonyl)-1H-indol-3-yl]acetic acids as potential COX-2 inhibitors. *Ind. J. Chem.* **2006**, *45B*,
723 2128–2132.
- 724 20. Sharma, P.; Kumar, A.; Pandey, P. A facile synthesis of N-phenyl-6-hydroxy-3-bromo-4-arylazo under
725 phase transfer catalytic conditions and studies on their antimicrobial activities. *Ind. J. Chem.* **2006**,
726 *45(B)*, 2077–2082.

- 727 21. Mladenova, R. ; Ignatova, M. ; Manolova, N. ; Petrova, T. ; Rashkov, I. Preparation, characterization
728 and biological activity of Schiff base compounds derived from 8-hydroxyquinoline-2-carboxaldehyde
729 and Jeffamines ED. *Eur. Polym. J.* **2002**, *38*, 989–999.
- 730 22. Kumar, A.; Kumar, D.; Akram, M.; Kaur, H. Synthesis and evaluation of some newer indole
731 derivatives as anticonvulsant agents. *Int. J. Pharm. Bio. Arch.* **2011**; *2*, 744–750.
- 732 23. Jayashree, B.S; Nigam, S; Pai, A.; Chowdary, P.V.R. Overview on the recently developed
733 coumarinylheterocycles as useful therapeutic agents. *Arabian. J. Chem.* **2014**, *7*, 885–899.
- 734 24. Xin-Mei, P. ; Guri, L.V.D. ; Cheng, H.Z. Current developments of coumarin compounds in medicinal
735 chemistry. *Curr. Pharm.* **2013**, *19*, 3884–3930.
- 736 25. Venugopala, K.N. ; Rashmi, V. ; Odhav, B. Review on natural coumarin lead compounds for their
737 pharmacological activity. *Bio. Med. Res. Int.* **2013**, *2013*, 1–14.
- 738 26. Sobhi, M.G.; Khaled, D.K. A Convenient Ultrasound-Promoted Synthesis of Some New Thiazole
739 Derivatives Bearing a Coumarin Nucleus and Their Cytotoxic Activity. *Molecules.* **2012**, *17*, 9335–9347.
- 740 27. Thoraya, A.F.; Maghda, A.A.; Ghada, S.M.; Zeinab, A.M. New and efficient approach for synthesis
741 of novel bioactive [1,3,4] thiadiazoles incorporated with 1,3-thiazole moiety. *Eur. J. Med. Chem.* **2015**, *97*,
742 320–333.
- 743 28. Singh, B.S.; Lobo, H.R.; Pinjari, D.V.; Jaraq, K.J.; Pandit, A.B.; Shankarling, G. S. Ultrasound and deep
744 eutectic solvent (DES): a novel blend of techniques for rapid and energy efficient synthesis of
745 oxazoles. *Ultrason. Sonochem.* **2013**, *1*, 287–293.
- 746 29. Bakht, M.A.; Ansari, M.J.; Riaydi, Y.; Ajmal, N.; Ahsan, M. J.; Shahar Yar, M. Physicochemical
747 characterization of benzalkonium chloride and urea based deep eutectic solvent (DES): A novel
748 catalyst for the efficient synthesis of isoxazolines under ultrasonic irradiation. *Mol. Liquid.* **2016**, *224*,
749 1249–1255.
- 750 30. Wang, S.Y.; Su, X.M.; A meldrum's acid catalyzed synthesis of Bis (Indolyl) methanes in water under
751 ultrasonic condition. *Chin. J. Chem.* **2008**, *26*, 22–24.
- 752 31. Zang, H.; Zhang, Y.; Cheng, B.W. An efficient ultrasound- promoted method for the one-pot synthesis
753 of 7,10,11,12-tetrahydrobenzo [C] acridin-8 (9) –one derivatives. *Ultrason. Sonochem.* **2010**, *17*, 495–499.
- 754 32. Imran, M.; Khan, S.A. Antiinflammatory activity of some new
755 3-(2H-1-benzopyran-2-one-3-yl)-5-substituted aryl isoxazolines. *Asian. J. Chem.* **2004**, *16*, 543–545.
- 756 33. El-Feky, H.A.S.; Imran, M.; Osman, A.N. Guanidine-annellated heterocycles: Design, synthesis and
757 biological evaluation of novel 2-aminopyridoimidazotriazines, pyridoimidazopyrimidines,
758 pyridoimidazotriazoles and pyridoimidazoles. *BAO. J. Pharm. Sci.* **2015**, *1*, 1–11.
- 759 34. Gupta, S.K.; Imran, M; Rehman, Z.U.; Khan, S.A. Synthesis and biological evaluation of some
760 2-substituted benzimidazoles. *Asian. J. Chem.* **2005**, *17*, 2741–2747.
- 761 35. Alam, O.; Gupta, S.K.; Imran, M.; Khan, S.A. Synthesis and biological activity of some
762 2,5-disubstituted 1,3,4-oxadiazoles. *Asian. J. Chem.* **2005**, *17*, 1281–1286.
- 763 36. Abbas, M.A. Synthesis of Sulfonyl 2-(prop-2-yn-1-yl thio)benzo [d] thiazole derivatives. *Al-Nahrain. J.*
764 *Sci.* **2015**, *18*, 74–78.
- 765 37. Mishra, D.; Fatima, A.; Rout, C.; Sing, R. An efficient one-pot synthesis of 2-aminothiazole
766 derivatives. *Der. Chem. Sin.* **2015**, *6*, 14–18.
- 767 38. Abdelriheem, N.A.; Mohamed, A.M.M.; Abdelhamid, A.O. Synthesis of some new 1,3,4-Thiadiazole,
768 Thiazole and pyridine derivatives containing 1,2,3-Triazole moiety. *Molecules.* **2017**, *22*, 1–15.
- 769 39. Bakht, M.A. Synthesis of some oxadiazole derivatives using conventional solvent and deep eutectic
770 solvent (DES) under ultrasonic irradiation: A comparative study. *Adv. Biores.* **2016**, *7*, 64–68.
- 771 40. Bakht, M.A. Ultrasound mediated synthesis of some pyrazoline derivatives using biocompatible deep
772 eutectic solvent (DES). *Der. Pharm. Chem.* **2015**, *7*, 274–278.
- 773 41. Pohle, T.; Brzozowski, T.; Becker, J.C.; VanderVoort, I.R.; Markmann, A.; Konturek, S.J.; Moniczewski,
774 A.; Domschke, W.; Konturek, J.W. Role of reactive oxygen metabolites in aspirin-induced gastric
775 damage in humans: gastroprotection by vitamin C. *Aliment. Pharmacol. Ther.* **2001**, *15*, 677–687.
- 776 42. Duggan, K.C.; Walters, M.J.; Musee, J.; Harp, J.M.; Kiefer, J.R.; Oates, J.A.; Marnett, L.J.
777 Molecular basis for cyclooxygenase inhibition by the non-steroidal anti-inflammatory drug naproxen.
778 *J. Biol. Chem.* **2010**, *285*, 34950–34959.

- 779 43. Lucido, M.J.; Orlando, B.J.; Vecchio, A.J.; Malkowski, M.G. Crystal Structure of Aspirin-Acetylated
780 Human Cyclooxygenase-2: Insight in to the Formation of Products With Reversed Stereochemistry.
781 *Biochem.* **2016**, *55*, 1226-1238.
- 782 44. Hou, T.J.; Zhang, W.; Xia, K.; Qiao, X.B.; Xu, X.J. ADME evaluation in drug discovery .5. Correlation
783 of caco-2 permeation with simple molecular properties. *J.Chem.Inf.Comput. Sci.* **2004**, *44*, 1585-1600.
- 784 45. Morris, C.J. Carrageenan-Induced Paw Edema in the Rat and Mouse, Inflammation Protocols: Dr John
785 Walker, editor. *Methods .Mol. Biol: Springer.* 2003,115-121.
- 786 46. Morris, C.J. Carrageenan-Induced Paw Edema in the Rat and Mouse, Inflammation Protocols: Dr John
787 Walker, editor. *Methods .Mol. Biol: Springer.* 2003,115-121.
- 788 47. Cioli, V. ; Putzolu, S. ; Rossi, V. ; ScorzaBarcellona, P. ; Corradino, C. The role of direct tissue contact
789 in the production of gastrointestinal ulcers by anti-inflammatory drugs in rats.
790 *Toxicol.Appl.Pharmacol.* 1979, *50*, 283-289.
- 791 48. Ohkawa, H.; Ohishi, N.; Yagi, K. Assay for lipid peroxides in animal tissues by thiobarbituric acid
792 reaction. *Anal. Biochem.* 1979, *95*, 351-358.
- 793 49. Anouar, E.; Calliste, C.; Kosinova, P.; Di Meo, F.; Duroux, J.; Champavier, Y.; Marakchi K.; Trouillas,
794 P.; Free radical scavenging properties of guaiacol oligomers: A combined experimental and quantum
795 study of the guaiacyl-moiety role. *J. Phys. Chem. A.* **2009**, *113*, 13881-13891.
- 796 50. Anouar, E.H. A Quantum Chemical and Statistical Study of Phenolic Schiff Bases with Antioxidant
797 Activity against DPPH Free Radical. *Antioxidants.* **2014**, *3*, 309-322.
- 798 51. Anouar, E.H.; Shah, S.A.A.; Hassan, B.; Moussaoui, N.E.; Ahmad, R.; Zulkefeli, M.; Weber, J.F.F.
799 Antioxidant Activity of Hispidin Oligomers from Medicinal Fungi: A DFT Study. *Molecules.* **2014**, *19*,
800 3489-3507.
- 801 52. Trucks, G.W.; Frisch, M.J.; Schlegel, H.B.; Scuseria, G.E.; Robb, M.A.; Cheeseman, J.R.; Scalmani,
802 G.; Barone, V.; Mennucci, B.; Petersson, G.A.; Nakatsuji, H.; Caricato, M.; Li, X.;
803 Hratchian, H.P.; Izmaylov, A.F.; Bloino, J.; Zheng, G.; Sonnenberg, J.L.; Hada, M.; Ehara, M.K.;
804 Toyota, R.F.; Hasegawa, J.; Ishida, M.; Nakajima, T.; Honda, Y.; Kitao, O.; Nakai, H.; Vreven, T.;
805 Montgomery, J.A.; Peralta, Jr. J.E.; Ogliaro, F.; Bearpark, M.; Heyd, J.J.; Brothers, E.;
806 Kudin, K.N.; Staroverov, V.N.; Kobayashi, R.; Normand, J.; Raghavachari, K.; Rendell, A.;
807 Burant, J.C.S.S.I.; Tomasi, J.; Cossi, M.; Rega, N.; Millam, J.M.; Klene, M.; Knox, J.E.; Cross,
808 J.B.; Bakken, V.; Adamo, C.; Jaramillo, J.; Gomperts, R.; Stratmann, R.E.; Yazyev, O.; Austin, A.J;
809 Cammi, R.; Pomelli, C.; Ochterski, J.W.; Martin, R.L.; Morokuma, K.; Zakrzewski, V.G.; Voth,
810 P.S.G.A.; Dannenberg, J.J.; Dapprich, S.; Daniels, A.D.; Farkas, O.; Foresman, J.B.; Ortiz,
811 J.C.J.V.; Fox, D.J. Gaussian 09 Revision A.02: **2009**.
- 812 53. Jacobson, M.P.; Friesner, R.A.; Xiang, Z.; Honig, B. On the Role of the Crystal Environment in
813 Determining Protein Side-chain Conformations. *J. Mol. Biol.* **2002**, *3220*, 597-608.
- 814 54. Jacobson, M.P.; Pincus, D.L.; Rapp, C.S.; Day, T.J.; Honig, B.; Shaw, D.E.; Friesner, R.A. A
815 Hierarchical Approach to All -Atom Protein Loop Prediction. *Proteins: Struct. Funct. Bioinf.* **2004**, *367*,
816 351-367.
- 817 55. Sastry, G.M.; Adzhigirey, M.; Sherman, W. Protein and ligand preparation : parameters protocols
818 and influence on virtual screening enrichments. *J.Comput. Aided.Mol.Des.* **2013**, *27*, 221-234.
- 819 56. Friesner, R.A.; Banks, J.L.; Murphy, R.B.; Halgren, T.A.; Klicic, J.J.; Mainz, D.T.; Repask, M.P.; Knoll,
820 E.H.; Shelley, M.; Perry, J.K.; Shaw, D.E.; Francis, P.; Shenkin, P.S. A new approach for rapid, accurate
821 docking and scoring 1. Method and assessment of docking accuracy. *J. Med .Chem.* **2004**, *47*, 1739-1749.
- 822 57. Friesner, R.A.; Murphy, R.B.; Repasky, M.P.; Frye, L.L.; Greenwood, J.R.; Halgren, T.A.; Sanschagrin,
823 P.C.; Mainz, D.T. Extra Precision Glide : Docking and Scoring Incorporation a Model of Hydrophobic
824 Enclosure for Protein -Ligand Complexes. *J. Med.Chem.* **2006**, *49*, 6177- 6196.
- 825 58. Halgren, T.A.; Murphy, R.B.; Friesner, R.A.; Beard, H.S.; Frye, L.L.; Pollard, W.T.; Banks, J.L .
826 Glide: A New Approach for Rapid, Accurate Docking and scoring .2. Enrichment Factors in Database
827 Screening. *J. Med. Chem.* **2004**, *47*, 1750-1759.

828 **Sample Availability:** Samples of the compounds are available from the authors.



© 2019 by the authors. Submitted for possible open access publication under the terms and conditions of the Creative Commons Attribution (CC BY) license (<http://creativecommons.org/licenses/by/4.0/>).

